May 24th - May 29th

A New Method for Evaluating Spatial Variability of Soil Strains Developed during Earthquakes Based on Electrical Resistivity Concepts Using Green's Function

Zhihua Li
AMEC Geomatrix, Inc., Oakland, CA


Fifth International Conference on
Recent Advances in Geotechnical Earthquake Engineering and Soil Dynamics
and Symposium in Honor of Professor I.M. Idriss
May 24-29, 2010 • San Diego, California

A NEW METHOD FOR EVALUATING SPATIAL VARIABILITY OF SOIL STRAINS DEVELOPED DURING EARTHQUAKES BASED ON ELECTRICAL RESISTIVITY CONCEPTS USING GREEN'S FUNCTION

Zhihua Li
AMEC Geomatrix, Inc.
Oakland, CA-USA 94612

ABSTRACT

A new method for evaluating spatial variability of soil strains during earthquakes is developed. The idea is based on electrical resisitivity concepts. By solving the classic Maxwell's equations applying Green's function for the boundary conditions, we obtained a closed form solution relating the electric potential measurements to the soil's displacements during earthquakes. The displacement information can be further used to obtain soil strains. In centrifuge models, the displacement measurements using an electrode switching system have been demonstrated to have spatial and temporal resolutions of 1 mm and 1 ms. Based on the high resolution of the displacement that is obtainable, strains of the soil matrix can be computed. The scheme of the method is to establish electromagnetic fields in saturated soil by injecting low-frequency alternating currents through electrodes in a designed mesh and the displacement of the soil is related to the change of electrical potential measured on the electrode located at that point. The viability of the technique is demonstrated by measuring the liquefaction-induced displacements of objects in a geotechnical centrifuge model test. This method is considered to be a useful technique for monitoring strain distributions in physical centrifuge models and has practical application potentials in the field.

INTRODUCTION

The soil stress-strain relationship constitutes the most fundamental frame of soil behavior. Therefore, strain, the study of deformation, plays a key role in establishing soil elastic-plastic models, obtaining soil modulus, and investigating soil properties. Soil strain can be measured in the triaxial apparatus for investigating the stress: strain behavior of a soil sample. Traditional monitoring of soil strain distribution is through strain gauges installed inside the soil medium. A common disadvantage of strain gauges is the sensitivity to temperature variations (Dunnicliff 1993).

This paper proposes a new electrical method to monitor soil strain development and evaluate soil strain distribution during a dynamic event, such as earthquake shaking. The idea of the method is to inject low-frequency alternating currents through electrodes in a designed mesh embedded inside the saturated soil to establish electromagnetic fields. Based on classic electromagnetism, the displacement of the soil is related to the change of electrical potential measured on the electrode located at that point. A closed-form solution was obtained based on Green's function to account for the particular boundary condition and a versatile high performance electrode switching system (ESS) (Li et al. 2006) has been implemented in a geotechnical centrifuge. Once the displacement is solved using the closed-form solution with the boundary condition accounted for, the strains in the mesh can be evaluated.

ELECTRICAL RESISTIVITY CONCEPTS

Resistivity (or resistance) measurement based on electromagnetic concepts provides an effective way to monitor spatial and temporal variations in soil for evaluating fundamental physical and mechanical properties of soil. Archie (1942) relates the in-situ electrical conductivity (the reciprocal of electrical resistivity) of sedimentary rock to its porosity and brine saturation

$$C_t = C_w \phi^m S_w^n \qquad (1)$$

Here, ϕ denotes the porosity, C_t is the electrical conductivity of the fluid saturated rock, C_w represents the electrical conductivity of the brine, S_w is the brine saturation, m is the cementation exponent of the rock (usually in the range 1.8–2.0), and n is the saturation exponent (usually close to 2). Soil resistivity has been shown empirically to depend on the resistivity of pore fluid, which saturates the particulate soil medium consisting of non-conductive particles, soil porosity, particle shape and size distribution, and the direction of measurements as

$$\rho_s = \rho_w \cdot n^{-\bar{f}} \tag{2}$$

where ρ_s is the resistivity of soil, ρ_w is the resistivity of pore fluid, n denotes soil porosity, and f is the form factor which is a function of the particle shape and grain size distribution, and has been shown empirically and theoretically to be independent on the porosity (Archie 1942; Arulanandan and Sybico 1992). $\bar{f}$ (usually around 1.0 ~ 2.4) is the average form factor, referring to the arithmetic average of form factors measured in three orthogonal directions. The ratio of the soil resistivity to the pore fluid resistivity is defined as the formation factor $F = \rho_s / \rho_w$, which has been used for determining volume changes during a pressuremeter test, for evaluating the in-situ porosity of non-cohesive sediments, and for evaluation of in-situ density and fabric of soil.

Other soil electrical measurements have been made possible based on the fundamental electromagnetic concepts, such as electrical resistivity tomography for monitoring contaminant evolution as a non-intrusive method (Günzel et al. 2003). Arulanandan et al. (1973, 1991) and Kutter et al. (1979) among others have proposed that formation factor, dielectric constant, and dielectric dispersion may be useful for measurement of porosity, soil type, anisotropy, and soil structure. Cho et al. (2004) and Li et al. (2005) describe a system for measuring resistivity profiles on a centrifuge using a needle probe and a robot. Versteeg et al. (2005) and Li et al. (2006) described a high speed resistivity measuring system and the implementation in a geotechnical centrifuge.

THEORY FOR ELECTRO-MONITORING SOIL STRAINS

Strain is the geometrical measure of deformation representing the relative displacement between particles in the material body, i.e. a measure of how much a given displacement differs locally from a rigid-body displacement. In a resistive medium, Initial locations and location changes (displacements) can be related to electrical potential measurements through introducing electromagnetic fields.

The time-harmonic forms of Maxwell's equations are

$$\nabla \times \mathbf{E} = -j\omega\mu \mathbf{H} \tag{3}$$

$$\nabla \times \mathbf{H} = \sigma \mathbf{E} + j\omega\varepsilon \mathbf{E} \tag{4}$$

where **E** and **H** represents the electric field and the magnetic field, respectively; and ω is the angular frequency.

The electric field **E** at a point is equal to the negative gradient of the electric potential V at that point

$$\mathbf{E} = -\nabla V \tag{5}$$

Assuming the soil is homogeneous, Equation (5) becomes Laplace's equation

$$\nabla^2 V = 0 \tag{6}$$

Solving Laplace's equation in spherical coordinates for a current source, I, at a point in an unbounded media with resistivity ρ, the potential V at a distance r from the injection point (Fig. 1), is as follows (with the aid of Ohm's law) (Dobrin and Savit 1988):

$$V = \frac{I\rho}{4\pi} \cdot \frac{1}{r} \tag{7}$$

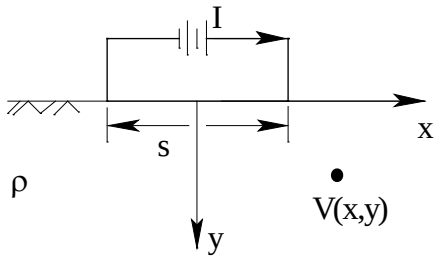

Fig. 1. Infinite half space with current injected from two surface electrodes.

If the soil medium occupies finite regions of space with prescribed boundary conditions on the bounding surfaces, which is the case in a model container, boundary conditions need to be accounted for. To handle general boundary conditions, it is necessary to apply Green's function *G (x,x')* which satisfies Laplace's equation

$$\nabla^2 G(x, x') = -\delta(x - x') \tag{8}$$

Green's function gives the potential at the point *x* due to a point charge at the source point *x'* and δ is the Dirac delta function. In cases when the medium is homogeneous and the boundaries are highly symmetric such as in rectangular containers, the classic method of images may be used to

satisfy the boundary conditions (Jackson 1998). The method of images originates from the replacement of certain elements in the original layout with imaginary charges, which replicates the boundary conditions of the problem. Figure 2 shows a sketch of the six first-order mirror images of a single real current source in the centrifuge model. Each imaginary image source (for an insulated boundary) is equal to the original real current source

$$I_i = I_0 \qquad i = 1, 2, \ldots, \text{n}, \ldots \tag{9}$$

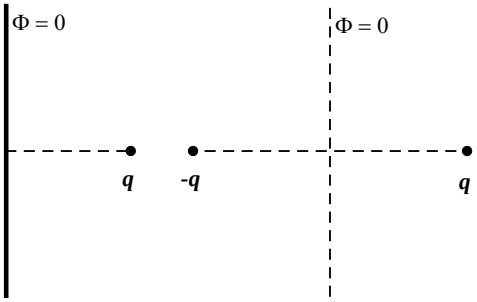

Fig. 2. Solution by method of images. The original potential problem is on the left, the equivalent-image problem on the right.

Therefore, the electric potential (voltage) V at a point of interest with distance r_i from I_i, is the summation of contributions of all the current sources (real source(s) and image sources) given by

$$V = \frac{I\rho}{4\pi} \cdot \sum_{i=0}^{\infty} \frac{1}{r_i} \qquad i = 1, 2, \ldots, \text{n}, \ldots \tag{10}$$

The potential derivatives with respect to coordinates x and z can be expressed as

$$\frac{\partial V}{\partial r} = -\frac{I\rho}{4\pi} \cdot \sum_{i=0}^{\infty} \frac{1}{r_i^2} \qquad i = 0, 1, \ldots, \text{n}, \ldots \tag{11}$$

Li and Kutter (2008) proposed an electro-location scheme which states that the displacements of the object in three dimensions can be determined through the known spatial derivatives of the potential by the following equation:

$$\begin{bmatrix} \Delta x \\ \Delta y \\ \Delta z \end{bmatrix} = \begin{bmatrix} \frac{\partial V_1}{\partial x} & \frac{\partial V_1}{\partial y} & \frac{\partial V_1}{\partial z} \\ \frac{\partial V_2}{\partial x} & \frac{\partial V_2}{\partial y} & \frac{\partial V_2}{\partial z} \\ \frac{\partial V_3}{\partial x} & \frac{\partial V_3}{\partial y} & \frac{\partial V_3}{\partial z} \end{bmatrix}^{-1} \begin{bmatrix} \Delta V_1 \\ \Delta V_2 \\ \Delta V_3 \end{bmatrix} \tag{12}$$

where Δx, Δy and Δz are the object displacements in three dimensions *x*, *y* and *z*; ΔV_i (i =1, 2 and 3) are the measured electrical potential changes due to the object displacements in three dimensions *x*, *y* and *z*; $\frac{\partial V_i}{\partial x}$, $\frac{\partial V_i}{\partial y}$ and $\frac{\partial V_i}{\partial z}$ (i =1, 2 and 3) are the spatial derivatives of electrical potentials with respect to *x*, *y* and *z*.

If the displacement is constrained to two dimensions in a vertical plane, Equation (12) reduces to

$$\begin{bmatrix} \Delta x \\ \Delta z \end{bmatrix} = \frac{1}{\left| \frac{\partial V_1}{\partial x} \cdot \frac{\partial V_2}{\partial z} - \frac{\partial V_1}{\partial z} \cdot \frac{\partial V_2}{\partial x} \right|} \begin{bmatrix} \frac{\partial V_2}{\partial z} & -\frac{\partial V_1}{\partial z} \\ -\frac{\partial V_2}{\partial x} & \frac{\partial V_1}{\partial x} \end{bmatrix} \begin{bmatrix} \Delta V_1 \\ \Delta V_2 \end{bmatrix} \tag{13}$$

Once the displacement is solved using the closed-form solution with the boundary condition accounted for, the strain can be computed. Strain defines the amount of stretch or compression along a material line elements or fibers, i.e. normal strain, and the amount of distortion associated with the sliding of plane layers over each other, i.e. shear strain, within a deforming body. The strain-displacement relationships can be summarized as

$$\varepsilon_{ij} = \frac{1}{2}\left(\frac{\partial u_i}{\partial x_j} + \frac{\partial u_j}{\partial x_i}\right) \tag{14}$$

where *u* is the displacement vector, *x* is the coordinate, and *i* and *j* can range over the three coordinates (1, 2, 3) in three dimensional space. Expanding the above equation for each coordinate gives

$$\begin{aligned} \varepsilon_{xx} &= \frac{\partial u}{\partial x} & \varepsilon_{yz} &= \frac{1}{2}\left(\frac{\partial w}{\partial y} + \frac{\partial v}{\partial z}\right) = \varepsilon_{zy} \\ \varepsilon_{yy} &= \frac{\partial v}{\partial y} & \varepsilon_{zx} &= \frac{1}{2}\left(\frac{\partial u}{\partial z} + \frac{\partial w}{\partial x}\right) = \varepsilon_{xz} \\ \varepsilon_{zz} &= \frac{\partial w}{\partial z} & \varepsilon_{xy} &= \frac{1}{2}\left(\frac{\partial v}{\partial x} + \frac{\partial u}{\partial y}\right) = \varepsilon_{yx} \end{aligned} \tag{15}$$

where *u*, *v* and *w* are the displacements in the *x*, *y*, and *z* directions respectively. The expression inside the parentheses can be rewritten as

$$\gamma_{yz} = \frac{\partial w}{\partial y} + \frac{\partial v}{\partial z} \quad \gamma_{zx} = \frac{\partial u}{\partial z} + \frac{\partial w}{\partial x} \quad \gamma_{xy} = \frac{\partial v}{\partial x} + \frac{\partial u}{\partial y} \tag{16}$$

where γ_{yz}, γ_{zx} and γ_{xy} are engineering shear strains.

If the displacement is constrained to two dimensions in a vertical *x*, *z*-plane, the strain-displacement relationships reduces to

$$\varepsilon_{xx} = \frac{\partial u}{\partial x} \qquad \varepsilon_{zx} = \frac{1}{2}\left(\frac{\partial u}{\partial z} \div \frac{\partial w}{\partial x}\right) = \varepsilon_{xz}$$
$$\varepsilon_{zz} = \frac{\partial w}{\partial z} \qquad \gamma_{zx} = \frac{\partial u}{\partial z} \div \frac{\partial w}{\partial x} \tag{17}$$

To monitor the evolution and distribution of soil strains during earthquakes in a geotechnical centrifuge model, change of electrical potential measured on embedded electrodes in a designed mesh inside saturated soil is evaluated while the low-frequency alternating currents are introduced to the boundary electrodes to establish electromagnetic fields. Fig. 3 shows a mesh of electrodes embedded in a centrifuge model container with dimensions 1.75 m by 0.64 m by 0.51 m. The spacing of electrodes in the mesh is 103 mm. Also shown is an example of electrode displacement in the *x*, *y*, and *z* directions.

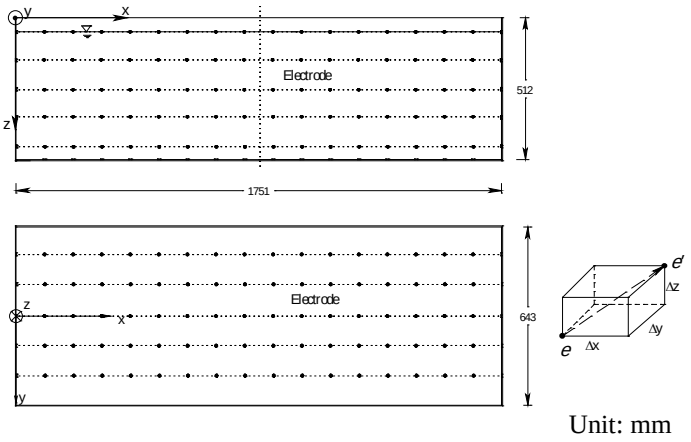

Unit: mm

Fig. 3. Electrode mesh in a centrifuge container. Top: side view; bottom-left: top view; bottom-right: displacement of an electrode (original position: e, final position: e').

In a two dimensional earthquake shake initiated in the geotechnical centrifuge, the electrode displacements are assumed to be constrained to two dimensions in a vertical *x*, *z*-plane.

In such case, the calculation of strains for an electrode $e_{i,j}$ as shown in Fig. 4 can be simplified as

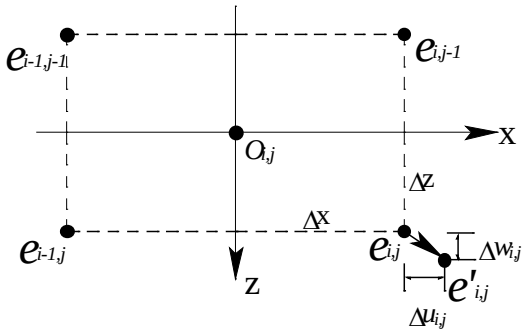

Fig. 4. Electrode displacements within an element of the designed mesh in the x, z-plane.

$$\varepsilon_{xx}\big|_{i,j} = \frac{\Delta u_{i,j}}{\Delta x}$$
$$\varepsilon_{zz}\big|_{i,j} = \frac{\Delta w_{i,j}}{\Delta z} \tag{18}$$
$$\gamma_{zx}\big|_{i,j} = \frac{\Delta u_{i,j}}{\Delta z} + \frac{\Delta w_{i,j}}{\Delta x}$$

where $\varepsilon_{xx}\big|_{i,j}$, $\varepsilon_{zz}\big|_{i,j}$, and $\gamma_{zx}\big|_{i,j}$ are strains developed at location of electrode $e_{i,j}$, $\Delta u_{i,j}$ and $\Delta w_{i,j}$ are displacements associated with electrode $e_{i,j}$ in the *x* and *z* direction respectively, and Δx and Δy are the distances of electrode $e_{i,j}$ to the center of the element $o_{i,j}$ in the mesh in the *x* and *z* directions respectively. Mesh dimensions Δx and Δy are constant throughout a uniform mesh.

Evaluation of strain distribution with respect to Cartesian coordinates in a heterogeneous bounded medium can be realized through solution of the Laplace equation using numerical analyses such as the finite element method or finite difference method.

INSTRUMENTATION AND CALIBRATION

Versteeg et al. (2005) described a high speed resistivity system for investigation of processes for geocentrifuges, capable of measuring 330,000 samples per second with 16-bit resolution, allowing high-speed sampling at 1 kHz without aliasing. This system was programmed to be implemented in the centrifuge as a versatile high-performance electrode switching system (Li et al. 2006). For calibration and resolution test, Fig. 5 shows a diagram of the electrode locations (N1-N5 (North), B1-B16 (Bottom), S1-S5 (South), T1 and T2 (Top)) inside a 1.75 m x 0.64 m x 0.51 m aluminum model container lined with a 3-mm-thick neoprene

sheet to isolate the conductive medium from the conductive container. The N, B, and S electrodes, consist of 9.5 mm diameter titanium plate attached at 103 mm spacing to the neoprene sheet. T1 and T2 consist of stainless steel bolts screwed into a plastic block suspended near the top of the container. The electrode switching system was used to inject electrical current $\pm I$ at electrodes N3 and S3 (as a horizontal pair), and at T1 and B7 (as a vertical pair), and measure the potentials on target electrode M (a 32-mm diameter stainless steel ball) submerged in a 0.01N NaCl solution. An algorithm to extract voltage values from a series of discrete raw data acquired using the electrode switching system is described and effects of sampling parameters based on signal processing theories are discussed in detail by Li (2006).

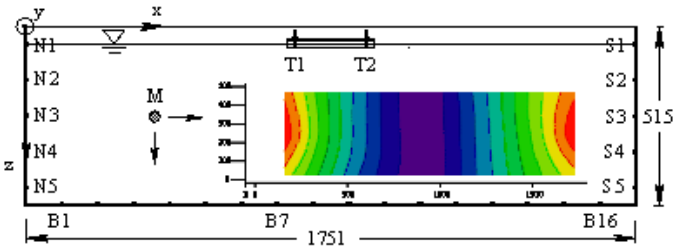

Unit: mm

Fig. 5. Schematic views of the calibration testing setup composed of the centrifuge container filled with 0.01 M NaCl solution, boundary electrodes and spherical target object, along with the coordinate system employed. Also shown is the electric potential contour (in color) due to current injection through N3-S3.

The resolution of the measurement was investigated experimentally and results are presented in Fig. 6. The actual sensitivity of the system was measured by moving the electrodes a small distance to determine the rate of change of position with respect to voltage $\Delta x/\Delta V$ and $\Delta z/\Delta V$. The horizontal resolution, for example, was then estimated as the product of the standard deviation of the voltage and the ratio $\Delta x/\Delta V$. Results show that with the increase of number of cycles per measurement, the resolution increases for both horizontal and vertical displacements. Also shown is that normally lower operating frequencies yield higher resolutions. With ten or more cycles per measurement, 1 mm resolution or even higher can be achieved at different frequencies.

An approximate equivalent circuit for the whole measurement setup including capacitors to represent the neoprene liner and capacitors to represent the imaginary conductivity of the medium is simulated. The equivalent transfer function for (voltage at M1 relative to B7)/(excitation current) is shown in Fig. 7. It indicates that the system behave as a low-pass filter with a corner frequency near 2 kHz. For desirable spatial and temporal resolutions, a set of sampling parameters is selected for measurement based on the parameter studies: 10 cycles per

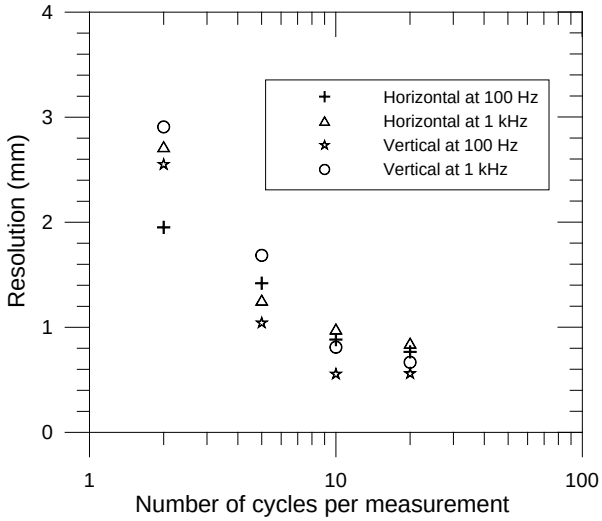

Fig. 6. Obtainable measurement resolutions for horizontal and vertical displacements.

measurement, 5 points per cycle (sampling frequency is 5 times the excitation frequency), 1 kHz excitation frequency and a cosine squared window function.

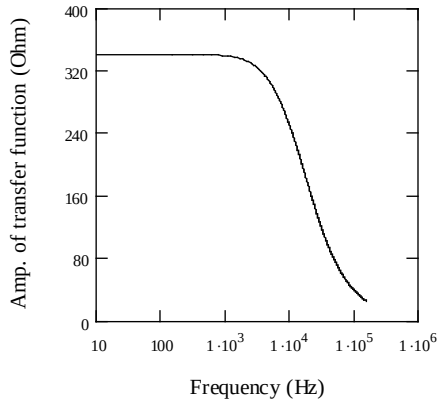

(a)

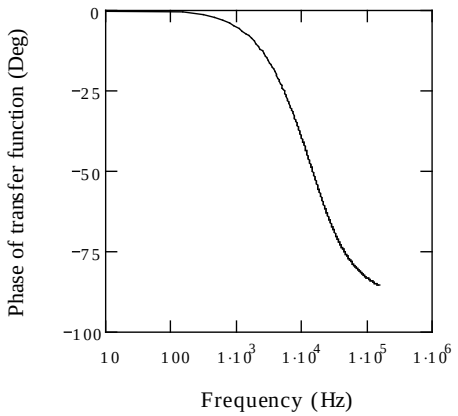

(b)

Fig. 7. Transfer function: (a) Magnitude; (b) Phase.

Obtainable spatial resolution is a function of the measurement duration and also varies with position within the medium. Theoretically, the spatial resolution can be estimated by multiplying the voltage resolution of A/D converter by the theoretical gradient of position with respect to voltage. For 16 bit conversion over a 10 volt range, the voltage resolution is $10 \times 2^{-16} = 1.5 \times 10^{-4}$ V. The theoretical gradient of position with respect to voltage is about 100 mm/V at a constant position (x, y, z) = (331, 0, 260). Therefore, the electro-location method using the electrode switching system should permit a spatial resolution of 0.015 mm. The significant discrepancy between the theoretical resolution (0.015 mm) and the experimental resolution (1 mm) may be due to wide-spectrum electrical noise and uncertain actual displacements of electrodes during the displacement-controlled calibration test, as opposed to the actual resolution of the electronics.

Using the selected sampling parameters, the potential fields and potential derivatives measured with 5 mA current source injected horizontally through N3 to S3 and vertically through T1 to B7, were compared with theoretically predicted values based on Equations (10) & (11) using the method of mirror images. The calculated potential fields and potential derivatives converge fast with respect to the increase of the number of image orders considered. By the time the fourth order mirror images are included, the calculated potential fields and derivatives already agree with third order image results, only differed by very small percentage discrepancies.

APPLICATON

Based on the high resolution of the displacement that is obtainable, this method can be applied in evaluating spatial variability of soil strains developed during dynamic events such as earthquakes. One of the difficulties in implementation is how to make sure each embedded electrode moves together with the soil medium surrounding it. In another word, the assumption is that the movement of the electrode "particle" is the movement of the soil particle the electrode replaces in that location. This can be achieved by selecting the material of the electrode of the density less or close to that of the surrounding soil medium. Aluminum electrodes satisfy this requirement. This scheme has not been implemented in the centrifuge models; however, the viability of the technique is demonstrated by measuring the liquefaction-induced displacements of objects with high resolutions in the geotechnical centrifuge model test.

Figure 8(a) shows a geotechnical centrifuge model containing a homogenous conductive soil medium with electrodes embedded to be monitored. The electrode groups N, B, S, and T are identical to those used in the calibration tests. To improve the resistivity homogeneity, the sand was washed and oven-dried, and then air-pluviated into the 0.01 M NaCl solution from a constant height above the surface of the water.

In this test six solid stainless steel spheres were included in the model. M1, M2, and M3 were half buried in the sand initially while M4, M5, and M6 were buried about 150 mm below the surface. These spheres were wired as electrodes to the electrode switching system so that the system could be used to measure their displacements when the ground was liquefied using the servo-hydraulic shaking table on the centrifuge. Note that this test served as a preliminary proof test of the method for detecting displacements and the heavy electrodes made of stainless steel were meant for significant displacements during earthquake-induced liquefaction. Fig. 8(a) also indicates that the model was instrumented with accelerometers (e.g.: A1),

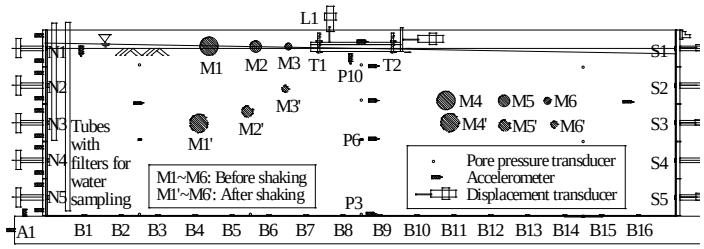

(a)

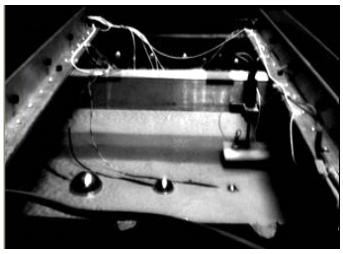

(b)

(c)

Fig. 8. Geotechnical centrifuge model test: (a) model with instrument layout for in-flight condition; (b) before shaking; (c) soil dissection after shaking. The final positions of the target objects from model dissection after the centrifuge testing are also shown in (a) (M1' ~ M6').

pore pressure transducers (e.g.: P3, P6, P10), displacement transducers (e.g., L1) to measure its dynamic response. Also notice a plastic tube with filter at the end along each of the two corner lines on the north end of the container was installed for pore fluid conductivity sampling at different phases of the testing. The pore fluid conductivity sampling confirmed that the conductivity was uniform and constant during the experiment.

Two major earthquake shakes at 30 g and 80 g of spinning (scaled versions of the motion measured at Santa Cruz in the 1989 Loma Prieta earthquake), respectively, were imposed on the model after full preparation. The shakes induced boiling and liquefaction inside the soil, and the spherical targets started to move horizontally and vertically in the soil medium. Using the proposed method with chosen sampling parameters, two current injections - horizontally through N3 to S3 and vertically through T1 to B7 were initiated throughout the

shaking events. Assuming the induced displacements were within vertical cross sections in the case of earthquake shakes initiated with the 2-D centrifuge shaker, two unknowns (x_i, z_i) were solved in two nonlinear equations for a set of vertical and horizontal current injections at time *i* using Newton's method in MATLAB:

$$f_V(x_i, z_i) = V_V(x_i, z_i) - \frac{I\rho}{4\pi} \cdot \sum_{j=0}^{n} \frac{1}{r_{Vj}(x_i, z_i)} \qquad (19)$$

$$f_H(x_i, z_i) = V_H(x_i, z_i) - \frac{I\rho}{4\pi} \cdot \sum_{j=0}^{n} \frac{1}{r_{Hj}(x_i, z_i)} \qquad (20)$$

where *f* is the real-valued function whose root(s) will be found using this iteration algorithm, subscripts $_V$ and $_H$ represent vertical and horizontal injection cases, *I*, ρ, and *V*, are the original current source, media resistivity, measured voltage at a distance r_j from each current source (including image sources). In this case, the total *n* current sources are considered. The known original positions of the targets are taken as the initial estimates.

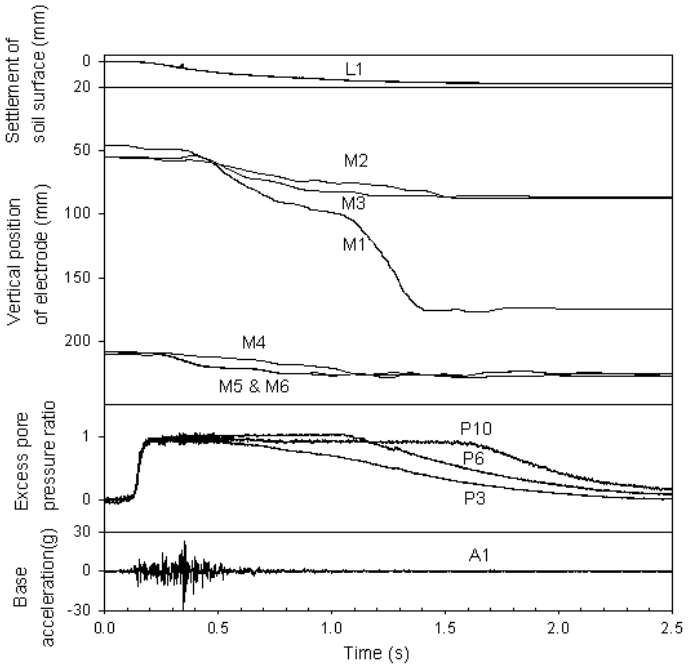

Fig. 9. Recorded response at 30 g in model scale.

Figure 9 shows the responses for Large Santa Cruz shake at 30 g in model scale by the time histories: soil surface settlement recorded by the top vertical potentiometer L1, calculated vertical positions of M1~M6, calculated excess pore pressure ratios based on records of the top, middle and bottom pore pressure transducers P10, P6 and P3 located at the center line, and the base acceleration recorded by A1, vs. time. We also obtained the actual total displacements by carefully excavating the model and measuring the locations before and after shakes (locations as shown in Fig. 8(b) and 8(c)). The calculated total vertical displacement of each electrode matches the actual value very well (along the 1:1 line); while the calculated total horizontal movements deviate from the actual ones. The discrepancies in the horizontal direction may be explained by the tilt deformations of the hinged plates on the two side walls at the "North" and "South" ends during the two major earthquake shakes.

The calculated relative displacements of the targets (location at time *i* minus location at time *i-1*) vs. time are shown in Fig. 10. Small relative displacements can be accurately detected.

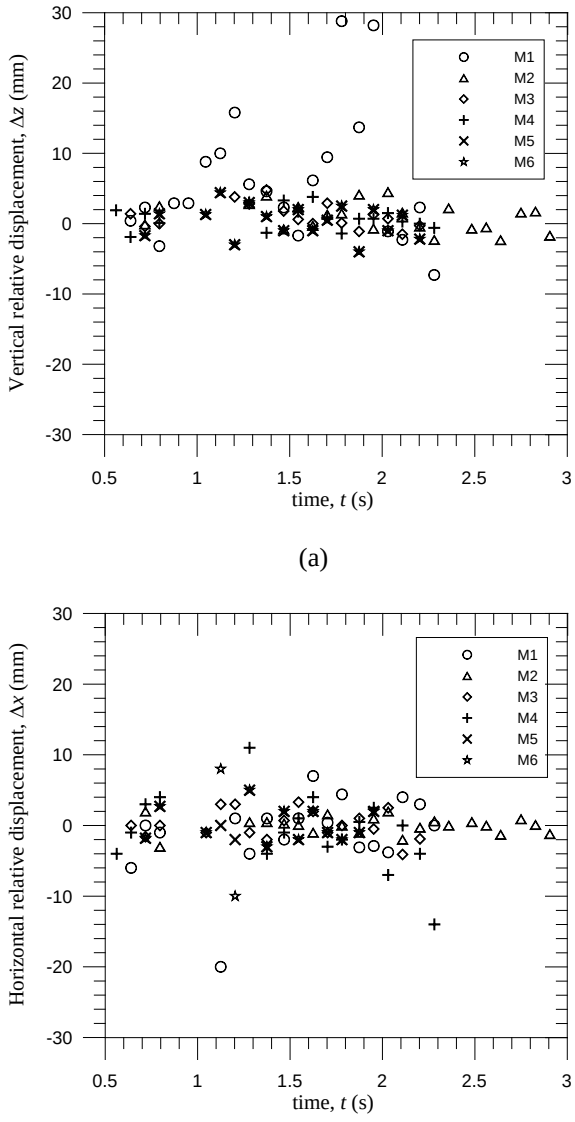

Fig. 10. Calculated relative displacement of M1~M6 (mm) (a) vertical, Δz ; (b) horizontal, Δx vs. time (s).

Though in this test, we didn't fully implement the scheme proposed as shown in Fig. 3, we believe that based on the high resolution results which agree remarkably with the actual values, the scheme of strain monitoring is viable and is possible to be fully implemented in the future.

CONCLUSIONS AND DISCUSSIONS

A new method for evaluating spatial variability of soil strains during earthquakes is proposed. The scheme of the method is to establish electromagnetic fields in a conductive medium (saturated soil) by injecting low-frequency alternating currents through electrodes in a designed mesh embedded inside the saturated soil and the displacement of the soil is related to the change of electrical potential measured on the electrode located at that point. Once the displacement is solved using the developed closed-form solution for potential distribution based on electrical concepts using Green's function, the strains in the mesh can be computed based on the fundamental strain concepts. The feasibility of the scheme is described through resolution study, calibration tests and actual displacement measurements during earthquake shakes in a centrifuge experiment with the employment of an electrode switching system with appropriate sampling parameters.

One of the biggest challenges using the proposed technique is to differentiate the measured voltage change caused by the medium conductivity change as the specimen strains, from the measured voltage change due to the electrode displacement along the surrounding soil medium. In more complicated situations of heterogeneous resistivity distribution, traditional electrical resistivity tomography can be employed for evaluation of spatial resistivity distribution to be applied in Equations (10) and (11). Displacements and strains can be monitored with application of numerical analyses involving finite element or finite difference schemes.

ACKNOWLEDGMENTS

This study is an extension of research which was supported by Award CMS-0086566 from the National Science Foundation under the Network for Earthquake Engineering Simulation (NEES) program. Prof. Bruce L. Kutter at University of California at Davis provided intellectual support and encouragement.

REFERENCES

Archie, G.E. [1942]. "The Electrical Resistivity Log as An Aid in Determining Some Reservoir Characteristics", Trans. Am. Inst. Min. Metall. Pet. Eng., Vol. 146, pp. 54-62.

Arulanandan, K. and S.S. Smith [1973]. "Electrical Dispersion in Relation to Soil Structure", Journal of Soil Mechanics and Foundation Division, ASCE, Vol. 99, pp. 1113-1133.

Arulanandan, K. [1991]. "Dielectric Method for Prediction of Porosity of Saturated Soil", Journal of Geotechnical and Geoenvironmental Engineering, ASCE, Vol. 117(2), pp. 319-330.

Arulanandan, K. and J. Sybico [1992]. "Post-liquefaction Settlement of Sands", *Proceedings of the Wroth Memorial Symposium*, Oxford University, England.

Cho, G. C., J.S. Lee, and J.C. Santamarina [2004]. "Spatial Variability in Soils: High Resolution Assessment with Electrical Needle Probe", Journal of Geotechnical and Geoenvironmental Engineering, Vol. 130(8), pp. 843-850.

Dobrin, M. and C.H. Savit [1988]. "*Introduction to Geophysical Prospecting (Fourth Edition)*". McGraw-Hill Book Company.

Dunnicliff, J. [1993]. "*Geotechnical Instrumentation for Monitoring Field Performance*". John Wiley & Sons, Inc.

Günzel, F., C. Fyfe and D.C.R. Davies [2003]. "Use of ERT in A Geotechnical Centrifuge", *3rd World Congress on Industrial Process Tomography*, Banff, Canada, pp. 607-612.

Jackson, J. D. [1998]. "*Classical Electrodynamics (Third Edition)*". John Wiley & Sons, Inc.

Kutter, B. L., K. Arulanandan.and Y.F. Dafalias [1979]. "A Comparison of Electrical and Penetration Methods of Site Investigation", *Offshore Technology Conference*, Houston, TX, pp. 1105-1115.

Li, Z. [2006]. "*Electro-location, Tomography and Porosity Measurements in Geotechnical Centrifuge Models Based on Electrical Resistivity Concepts*". PhD thesis, University of California, Davis.

Li, Z. and B.L. Kutter [2008]. "A New Technique for Monitoring Movement of Buried Objects Using an Electrode Switching System", Geotech. Testing Journal, ASTM, Vol. 31(5), pp. 381-393.

Li, Z., B.L. Kutter, D. LaBrecque and R. Versteeg [2006]. "A New Electrode Switching System (ESS) and a Scheme for Measurement of the Movement of Buried Objects", 6th International Conference on Physical Modeling in Geotechnics, 2006, Hong Kong, China.

Li, Z., B.L. Kutter, D.W. Wilson, K. Sprott, J.S. Lee and J.C. Santamarina [2005]. "Needle Probe Application for High-resolution Assessment of Soil Spatial Variability in the Centrifuge", *ASCE GeoFrontiers 2005*, Austin, TX.

Versteeg, R., D. LaBrecque, B.L. Kutter, E. Mattson, A. Richardson, R. Sharpe, Z. Li, D. Wilson and A. Stadler [2005]. “A High Speed Resistivity System for Investigation of Processes on Geocentrifuges”, *ASCE GeoFrontiers 2005*, Austin, TX.